Application Note

Cell Health and Viability

Agilent

Trusted Answers

Automated Kinetic Imaging Assay for Quantifying Cell Health

Agilent BioTek Cytation 9 with BioSpa 8 delivers richer, time-resolved insights for high-throughput analysis of cell proliferation and viability

Authors

Rebecca Mongeon, PhD
Joe Clayton, PhD
Agilent Technologies, Inc.

Abstract

Long-term, high-throughput monitoring of cell proliferation and viability is critical to understanding drug effects and cellular mechanisms of action. Endpoint assays for measuring cell health typically rely on indirect readouts and provide limited insights, while conventional image-based approaches can be hindered by environmental stability, focus drift, multiplexing capacity, and analytical complexity. To address these challenges, we implemented an automated kinetic workflow using the Agilent BioTek Cytation 9 cell imaging multimode reader, which delivers advancements in imaging speed, wide-field image quality, laser autofocus stability, and environmental control. Pairing the Cytation 9 instrument with the Agilent BioTek BioSpa 8 automated incubator allowed for fully unattended, extended live-cell studies. Integrated Agilent BioTek Gen5 software handled image acquisition and analysis, streamlining multiparametric workflows, and accelerating data interpretation.

In this proof-of-concept study, HT-1080 cells in 96- and 384-well formats were monitored using a multimode label-free and fluorescence imaging strategy that combined brightfield imaging with multiplexed viability stains. Fully automated imaging every two hours for four days enabled longitudinal quantification of cell health and dose-response analysis, including IC_{50} determinations across proliferation, early apoptosis, and irreversible cell death. This workflow revealed distinct kinetic signatures across multiple antineoplastic compounds, capturing cytostasis, apoptotic activation, lytic cell death, and delayed cytotoxic responses with high sensitivity.

Introduction

Regulated cell death is fundamental to proper tissue development and maintenance, and dysregulation contributes to a wide range of diseases. A major challenge in oncology involves malignant cells avoiding or delaying commitment to programmed cell death pathways during therapeutic intervention.[1] Whether driven by chemotherapeutics, targeted agents, or immunomodulatory treatments, many cancer therapies aim to push cancer cells into committed and irreversible cell death. The development of sensitive and reliable approaches to monitor cell growth and viability is essential to drug discovery, basic research, and translational studies. Understanding the molecular events that define the transition into irreversible cell death—and the mechanisms cancer cells use to resist them—continues to be an important focus in these fields.

Advances in live-cell imaging have enabled continuous monitoring of cell death processes and improved the characterization of the signals leading to cell death. One hallmark of early apoptosis is the externalization of phosphatidylserine (PS) from the inner to the outer leaflet of the plasma membrane.[2] In this study, early apoptotic PS exposure was visualized using the eAnnexinV Green fluorescent probe, which increases in fluorescence upon binding and provides a real-time indicator of apoptotic pathway activation.[3] When paired with label-free measurements of proliferation, these readouts offer a more complete picture of how cells grow, respond to treatment, and move toward irreversible cell death.

Loss of membrane integrity typically occurs in later stages of cell death and marks a key transition point.[4] This change can be detected through nuclear uptake of membrane-impermeant dyes such as propidium iodide (PI), allowing real-time visualization of irreversible cell death. Integrating early apoptotic indicators with late-stage commitment markers creates a multiparametric approach that provides richer insight than traditional endpoint measurements.

Because cell death is a continuous process that unfolds over time, kinetic imaging offers a more complete picture of treatment responses. Long term imaging reveals the timing, rate, and sequence of cell responses, supporting studies focused on drug mechanism of action, treatment sensitivity, and recovery potential. However, extended live-cell imaging in high-throughput studies requires maintaining environmental stability, preventing focus drift, and preserving image quality throughout the experiment.

Here we demonstrate a powerful proliferation and viability assay approach combining long-term label-free and fluorescence imaging in both 96- and 384-well microplate formats (Figure 1). The Cytation 9 cell imaging multimode reader combines multichannel fluorescence and brightfield imaging with laser autofocus for reliable, high-quality image acquisition over extended periods. The wide-field-of-view camera and enhanced imaging speed streamlines high-content kinetic workflows. Integration with the BioSpa 8 automated incubator supplied stable environmental control and fully unattended operation, enabling robust, long-term kinetic imaging in a high-throughput format.

Experimental

Materials

Reagents

All chemicals were obtained from Sigma Aldrich unless otherwise noted, including methotrexate (p/n A6770), Hoechst 33342 (p/n B2261), and propidium iodide (p/n P4170). Staurosporine (p/n 1285), vinblastine (p/n 1256), and nocodazole (p/n 1228) were obtained from Tocris Biosciences. eAnnexinV Green was obtained from Agilent Technologies (p/n 8711006).

Cell culture

HT-1080 fibrosarcoma cells were obtained from ATCC (p/n CCL-121) and cultured in Advanced DMEM medium (Thermo Fisher Scientific, p/n 12491015) supplemented with 10% FBS, 1x GlutaMAX (Thermo Fisher Scientific, p/n 35050061) and primocin antibiotic (InvivoGen, p/n ant-pm-1). Cells were maintained at 37°C in a humidified incubator with 5% CO_2 environment and routinely passaged at ~ 80% confluency. For proliferation and viability assays, HT-1080 cells were plated in 96-well (Corning, p/n 3904) and 384-well (Revvity, p/n 6057600) microplates.

Instrumentation

A Cytation 9 multimode imaging reader was equipped with the following accessories: 4x Plan Extended Apochromat objective (p/n 1220573), 10x Plan Fluorite objective (p/n 1220518), DAPI filter and LED cube (p/n 1225100 and p/n 1225013), GFP filter and LED cube (p/n 1225101 and p/n 1225001), propidium iodide filter and LED cube (p/n 1225111 and p/n 1225003) and laser autofocus option.

Methods

Cell culture and assay setup

For assay seeding, HT-1080 cells were harvested, and cell suspensions were added to a final count of ~ 500 and ~ 1,000 cells per well in 384- and 96-well plates, respectively. Plating media included Hoechst 33342 (30 nM) to allow sufficient time for label uptake and equilibration. Plated cultures were left for 30 minutes at room temperature to adhere and maintain even dispersal in the well before transferring to the tissue culture incubator. After overnight incubation (~ 14 hours), plates were removed from the incubator and media prepared with test compounds, and viability indicators were applied. eAnnexinV Green was applied to cultures at a final concentration of 0.25 µg/mL (1:200 dilution) and propidium iodide was applied to cultures at a final concentration of 1.5 µM. Imaging commenced directly after test compounds and viability indicators were applied.

System overview and environmental management

For fully automated, long-term imaging, the Agilent BioTek Cytation 9 instrument was integrated with the BioSpa 8 automated incubator. The BioSpa 8 maintained long-term environmental conditions of 37 °C with 5% CO_2 gas level in a humidified chamber with up to eight-plate capacity. Agilent BioTek BioSpa OnDemand software coordinated the scheduled delivery of both 96- and 384-well microplates to the Cytation 9 instrument at the specified imaging interval for several days. During active imaging periods, the Cytation 9 maintained environmental conditions (37 °C and 5% CO_2) with adjustable onboard controls in Gen5 software.

Automated image capture and processing

For simultaneous proliferation and viability analysis, kinetic image of HT-1080 cultures in 96- and 384-well plates were acquired every two hours for four days on the Cytation 9 and BioSpa 8 live-cell analysis platform. Images were captured at the center of the well at 4x magnification for three fluorescence channels, high-contrast brightfield, and a defocused (–300 µm offset) high-contrast brightfield image used for cell counting analysis. Images were also collected at 10x magnification in three fluorescence channels and standard brightfield modes for more detailed morphological observations.

Image and data analysis

Gen5 software was used for all image acquisition and analysis. Gen5 software Cellular Analysis steps were used to determine cell counts across all image channels including label-free, nuclear labeled, eAnnexinV, and PI images. The settings used to identify cells in each channel are provided in Table 1. Following image analysis, downstream analytical data tools in Gen5 software provided normalization, kinetic calculations (e.g., area-under-the-curve integration), maximum growth rate determination, doubling time, and dose-response analysis. Additional statistical analysis was performed in Prism Graphpad software.

Table 1. Agilent BioTek Gen5 software settings for Cellular Analysis steps.

Parameter	Label-Free Cell Count	Nuclear Cell Count	eAnnexinV+ Cell Count	PI+ Cell Count
Primary Mask				
Detection Channel	Bright Field: High Contrast[2]	DAPI	GFP	Propidium Iodide
Threshold	6000	3000	6000	8000
Background	Dark	Dark	Dark	Dark
Split Touching Objects	Yes	Yes	Yes	Yes
Fill Holes in Masks	Yes	Yes	Yes	Yes
Minimum Object Size	8	5	15	7
Maximum Object Size	100	100	100	100
Include Primary Edge Objects	**Yes**	**Yes**	**Yes**	**Yes**
Analyze Entire Image	Yes	Yes	Yes	Yes
Advanced Detection Options				
Rolling Ball Diameter	20	30	30	30
Image Smoothing Strength	5	1	3	2
Evaluate Background On	5	5	5	5
Primary Mask	Use threshold mask	Use threshold mask	Use threshold mask	Use threshold mask

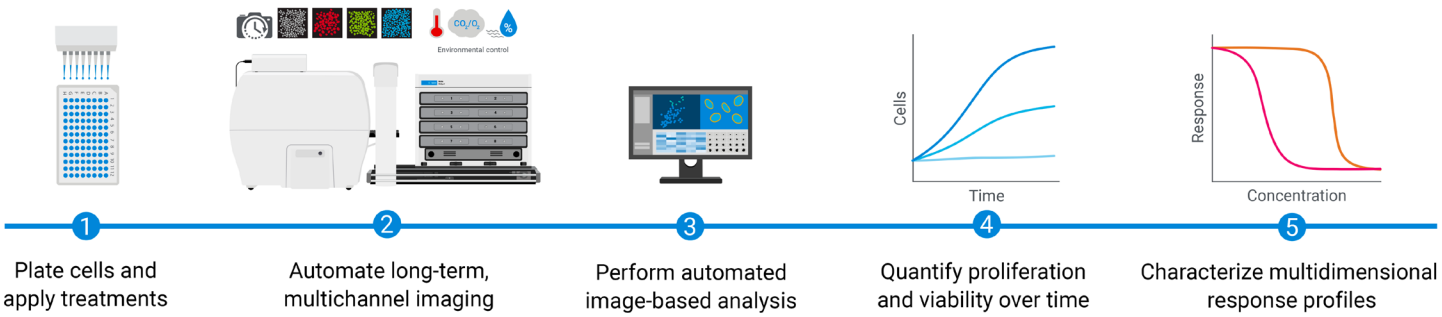

Figure 1. General proliferation and viability assay workflow on the Agilent BioTek Cytation 9 multimode imaging reader and BioSpa 8 automated cell incubator. Assay plates are seeded with relevant cellular models and treatments and viability indicators are applied just before imaging commences. The BioSpa8 automated incubator delivers plates to the Cytation9 for automated multiplexed imaging and analysis over time. Gen5 software provides analytical tools for detailed kinetic proliferation and viability analysis, yielding quantitative insight into treatment profiles.

Results and discussion

Workflow overview

Figure 1 shows a general assay setup and workflow for automated proliferation and viability analysis on the Cytation 9 automated imaging reader and integrated BioSpa 8 automated incubator. In this proof-of-concept study, HT-1080 fibrosarcoma cells were plated and evaluated in 96- and 384-well plate high-throughput formats. Cultures were treated with multiple antineoplastic drugs applied across a seven-point concentration series, and fluorescent viability indicators were applied to track cell death mechanisms over time. Multichannel images, including label-free brightfield images, were automatically collected at two-hour intervals for several days. The Cytation live-cell analysis platform leveraged Gen5 software for integrated image acquisition and downstream analysis, including cell segmentation, feature extraction, kinetic plotting, integral analysis, and dose-response evaluation.

Confluence-based cell proliferation analysis

Confluence-based evaluations provide a simple measure of population growth without labels. Human estimates of confluence can vary, whereas automated image-analysis based quantitation of confluence can provide an objective and reproducible measure of population growth over time. In Figure 2, example brightfield images and corresponding confluence analysis are depicted for HT-1080 cell culture over time for the Cytation 9 imager and Gen5 software analysis. Using this approach, drug-induced effects in percent confluence can be evaluated and compared over time (Figure 2D). However, confluence only provides a relative guide to population growth and is not equivalent to a true count of cells over time, limiting its utility in multiplexed, high-throughput investigations.

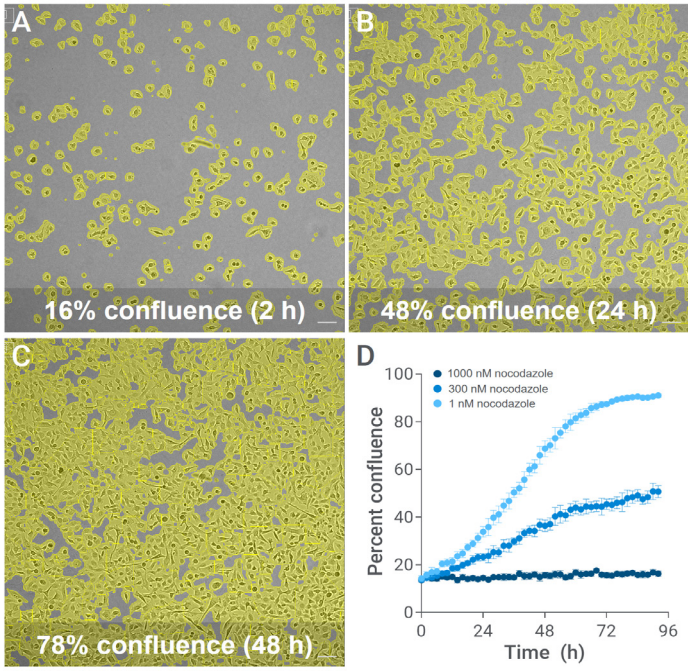

Figure 2. Evaluating proliferation through confluence measurements. (A–C) Example high-contrast brightfield images of HT-1080 cell cultures captured at 4x magnification on the Cytation 9. Automated Gen5 software image analysis determines the area occupied by cells (yellow overlay) and resultant percent confluence calculation for each image. Scale bars correspond to 100 µm. (D) The percent confluence over time is plotted for HT-1080 cells exposed to varying concentrations of nocodazole, indicating decreasing confluence with increasing doses. Data points represent mean and standard deviation of replicate wells (n = 12).

Cell counting-based cell proliferation analysis

Single-cell identification over time supports quantitative population-level analysis for proliferation assays. Cytation 9 instruments (and Gen5 software) support both labeled and label-free methods for cell counting through multiplexed imaging and analysis (Figure 3). HT-1080 cells were cultured in 30 nM Hoechst 33342 for nuclear labeling and determination of cell count over time (Figure 3A–C). Nuclear labels are often preferred for cell enumeration, as they often provide clearer cell separation than cytosolic labels. Gen5 image analysis software segments and provides individual nuclear counts from nuclear-labeled images (Figure 3C).

The Cytation 9 also supports label-free cell counting through the High-Contrast Brightfield Cell Counting technique, as shown in Figure 3. High-contrast brightfield images are collected in focus (Figure 3D) as well as defocused to provide a high-contrast cell image for cell counting (Figure 3E). Gen5 software automatically detects and counts cells in the high-contrast cell image (Figure 3F). Cell counts are comparable between nuclear and label-free methods for HT-1080 cells over a 96-hour proliferation assay (Figure 3G). Cell counts can be further analyzed in Gen5 software to determine population doubling time (Figure 3H), where analysis of nuclear and label-free counts both yield a 16-hour maximal doubling time estimate for HT-1080 cells.

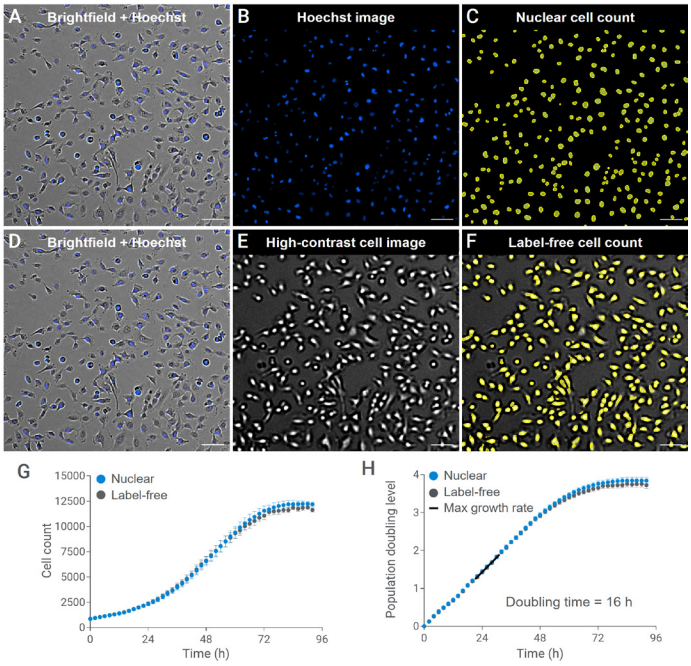

Figure 3. Evaluating proliferation through fluorescence and label-free cell counting techniques. (A) Example overlay of brightfield and Hoechst 33342 fluorescence nuclear staining in live cells captured at 4x magnification. (B) Hoechst staining (30 nM final concentration) provides a reliable way to label nuclei over time in live cells. (C) Agilent BioTek Gen5 data analysis software automatically identifies individual nuclei from low-magnification images (yellow overlay) and reports cell counts over time. (D) Example overlay of brightfield and Hoechst fluorescence nuclear staining in live cells captured at 4x magnification. (E) Capture of a defocused high-contrast brightfield image on the Agilent BioTek Cytation 9 cell imaging multimode reader provides a means of label-free cell quantification. (F) Gen5 software automatically detects individual cells (yellow overlay) from high-contrast cell counting images. (G) Plotting cell counts over time in HT-1080 cell culture demonstrates highly comparable results using nuclear staining (blue) and high-contrast cell counting techniques (grey). Data points represent mean and standard deviation for replicate wells (n = 10). (H) Further evaluation of growth rate through population doubling and maximum rate analysis in Gen5 yields doubling time estimates of 16 hours for HT-1080 cells using either label or label-free approaches. Data points represent mean and standard deviation for replicate wells (n = 10). Scale bars correspond to 100 µm.

Multiplexed cell viability indicator analysis

Cell proliferation is often a sensitive indicator of drug effect, as it is a high-level, integrative readout of cellular processes. Coupling cell proliferation with multiplexed viability readouts provides in-depth insights into treatment effects that cannot easily be captured through proliferation alone. Here we combine cell proliferation with markers of cell viability for multiplexed, high-throughput, kinetic live-cell analysis.

Three live-cell fluorescent indicators were combined with label-free analysis for evaluation of HT-1080 responses to a panel of antineoplastic drugs (Figure 4). First, Hoechst 33342 was applied nuclear segmentation and total cell marker (Figure 4A and E). Hoechst 33342 accumulates in both live and dead cells, providing a total cell readout over time. Second, eAnnexinV Green was applied as an indicator of early apoptosis (Figure 4B and F). eAnnexinV Green binds phosphatidylserine, normally found on the inner leaflet of cell plasma membranes and reports on membrane inversion events during early apoptosis. Finally, propidium iodide (PI) was applied as an indicator of irreversible, committed cell death (Figure 4C and G). PI only enters cells when membrane integrity is lost, providing an indicator for committed and irreversible cell death. Together, multiplexed live-cell cell indicators paint a detailed picture of cell proliferation and death mechanisms over time.

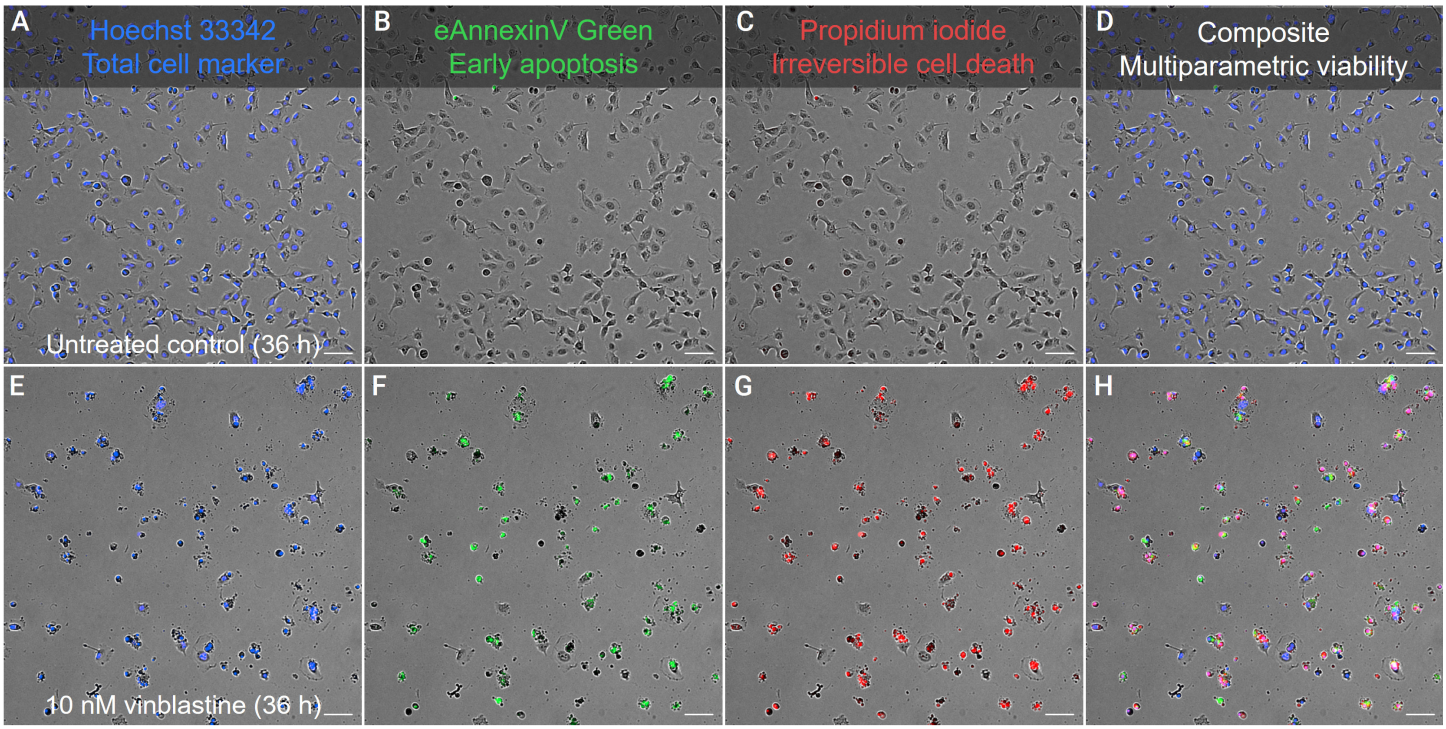

Figure 4. Fluorescence readouts from eAnnexinV and PI signals analysis reveal cytotoxic mechanisms in live-cell assays. (A and E) Live-cell staining with Hoechst 33342 (30 nM) provides a marker for nuclear segmentation and total cell counts. Hoechst staining is retained in both untreated HT-1080 cells shown in panel A and condensed nuclei of cells responding to cytotoxic treatment in panel E. (B and F) eAnnexinV Green labels early apoptotic cells, providing insight into early membrane inversion events related to apoptotic pathway activation. Untreated HT-1080 cell cultures shown in panel B present little to no eAnnexinV Green staining, while cytotoxic treatment in panel F shows significant staining. (C and G) Propidium iodide (PI) is an established marker for late apoptosis and necrosis events, reporting membrane rupture and committed cell death. Untreated HT-1080 cells in panel C exclude PI, while treated cells shown in G label brightly with PI. (D and H) Composite image overlay of Hoechst, eAnnexinV Green, and PI staining. Scale bars correspond to 100 µm.

Simultaneous kinetic profiling of proliferation and cell death mechanisms

Automated, multiplexed imaging was performed over time in HT-1080 cell cultures on the Cytation 9 cell imaging multimode reader with BioSpa 8 automated incubator. Proliferation curves were generated from cell counts over time and averaged across replicates (Figure 5A). eAnnexinV Green-positive cells were identified in Gen5 software through image analysis, and the percentage of positive cells was evaluated over time (Figure 5B). Similarly, PI-positive cells were identified, quantified, and plotted as the percentage of positive cells over time (Figure 5C).

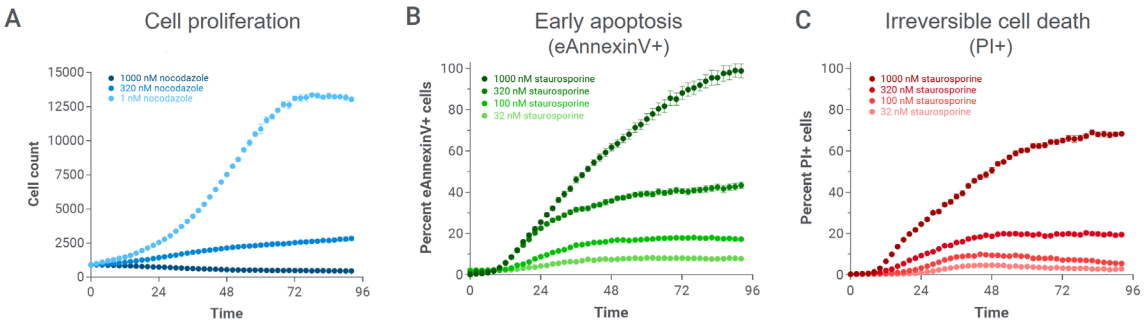

Figure 5. Kinetic analysis of cell counts and normalized viability indicators. (A) Proliferation curves evaluated across multiple concentrations of the drug nocodazole. Data points represent the mean and standard deviation of replicate wells (n = 3). (B) Percentage of cells positive for the apoptosis marker eAnnexinV Green evaluated across four concentrations of the drug staurosporine. Data points represent the mean and standard error of replicate wells (n = 10). (C) Percentage of cells positive for the committed cell death marker PI for four concentrations of the drug staurosporine. Data points represent the mean and standard error of replicate wells (n = 10).

Signature cytotoxic response profiles across treatments

The Agilent BioTek automated platform for simultaneous multiplexed cell proliferation and viability analysis revealed specific profiles across several example antineoplastic treatments (Figure 6). Untreated control HT-1080 cultures rapidly proliferated with negligible percentages of cells positive for apoptotic or committed cell death signals (Figure 6A and E). Treatment with staurosporine resulted in significant and rapid apoptosis, with relatively delayed committed cell death (Figure 6B and F). Nocodazole treatment initiated rapid general cytotoxicity presenting as concomitant increases in both lytic cell death and apoptotic signals (Figure 6C and G). Following membrane rupture, both PI and eAnnexinV Green enter and co-label cells. The methotrexate treatment profile highlighted cytostasis and growth arrest as the primary effect, without concomitant increases in apoptosis or cell death. This is consistent with methotrexate's cell cycle inhibition through repression of purine synthesis and resultant S-phase arrest.[5]

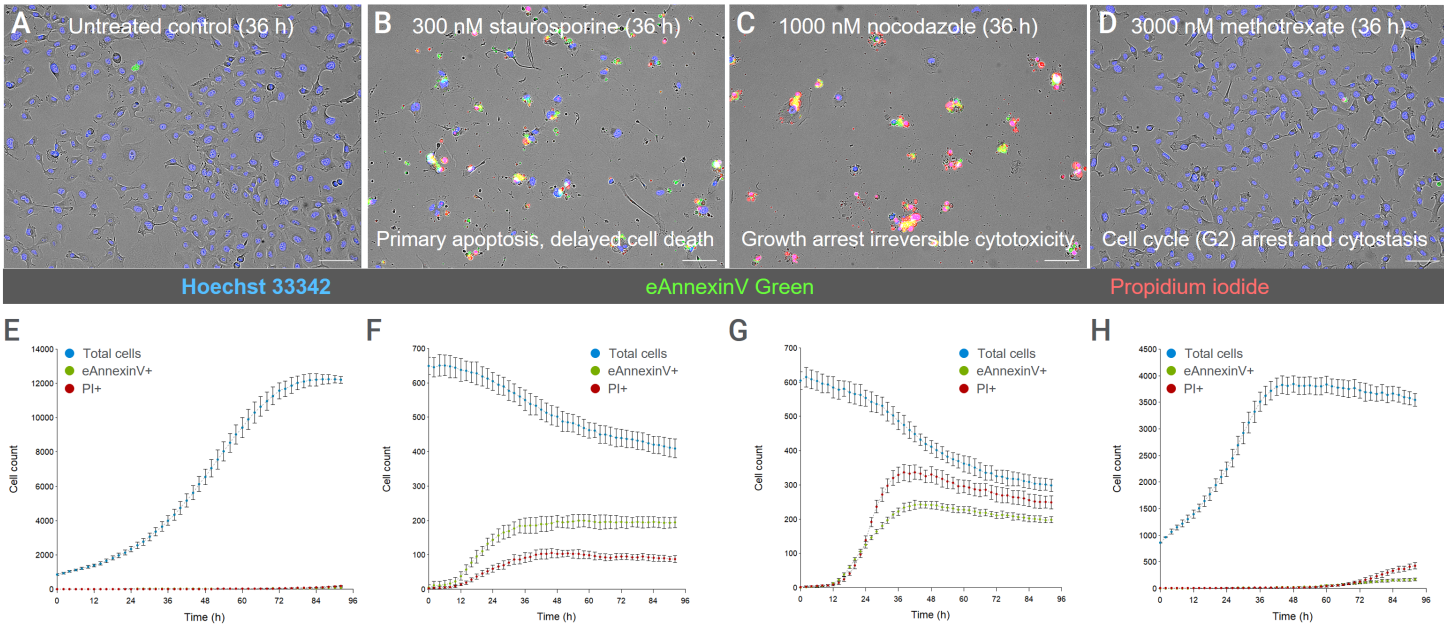

Figure 6. Continuous multiplexed outputs reveal unique drug response profiles over time. (A and E) Example image in A is composite overlay of brightfield and multichannel fluorescence images for untreated HT-1080 cell cultures at 10x magnification. Example images are shown from the 36-hour timepoint that corresponds to peak drug response timing across treatments. Corresponding kinetic proliferation and viability marker analysis shown in panel E for untreated HT-1080 cell cultures. Data points indicate mean and standard deviation of replicate wells (n = 8). (B and F) Example image in panel B depicts representative staurosporine response including loss of proliferation and increased apoptotic and cell death signal. Panel E shows the corresponding kinetic analysis for proliferation and viability markers for the same concentration of staurosporine depicted in panel B. Data points indicate mean and standard deviation of replicate wells (n = 10). (C and G) Example image in panel C depicts representative nocodazole response including loss of proliferation and increased apoptotic and cell death signal. Panel G depicts the corresponding kinetic analysis for proliferation and viability markers for the same concentration of nocodazole depicted in panel C. Data points indicate mean and standard deviation of replicate wells (n = 10). (D and H) Example image in panel D depicts representative methotrexate response including initial proliferation, plateaued growth, and without coincident cell death. Panel H depicts the corresponding kinetic analysis for proliferation and viability markers for the same concentration of methotrexate depicted in panel D. Data points indicate mean and standard deviation of replicate wells (n = 3). Scale bars correspond to 100 µm.

Delayed and low-dose exposure effects

The primary drug effects presented in Figure 5 across multiple drugs were complemented by the analysis of delayed and low-dose exposures of the same drugs (Figure 7). While untreated control HT-1080 cells proliferated to full confluence (Figure 7A), prolonged exposure or lower concentrations of drugs resulted in several secondary effects that were captured. Low nanomolar concentrations of staurosporine resulted in decreased proliferation and significant changes in cell morphology (Figure 7B). Similarly, lower doses of nocodazole also resulted in decreased proliferation with morphology changes (Figure 7C). At late time points, methotrexate exhibited delayed cytotoxicity in response to continued cell cycle arrest (Figure 7D).

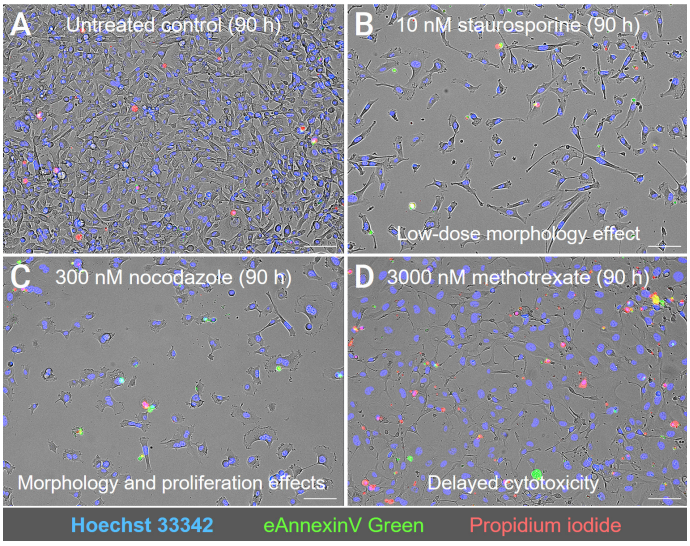

Figure 7. Kinetic imaging captures delayed and low-dose treatment effects. (A) Example multichannel composite image of untreated HT-1080 cells at late time points where growth has reached full confluency. (B) Corresponding timepoint image of very low-dose staurosporine treatment demonstrates effects on cell proliferation and morphology, but minimal apoptosis or cell death. (C) Long-term exposure to lower doses of nocodazole captures effects on morphology and proliferation. (D) Concentrations of methotrexate that primarily result in cell cycle arrest exhibit delayed cytotoxicity at later timepoints. Scale bars correspond to 100 µm.

Quantifying dose-dependence on proliferation and viability

Although kinetic profiles provide detailed insight into relevant measurements over time, deeper pharmacological insights require additional dose-response analysis. Kinetic curves for both cell count and viability signals are quantified through integral analysis, providing area-under-the-curve (AUC) values for dose-response analysis. Figure 8 depicts side-by-side dose-response analysis for proliferation, early apoptosis, and irreversible cell death measurements for four antineoplastic drugs.

Dose-response evaluation revealed cell proliferation (Figure 8A) was the most sensitive measure of drug effect, yielding the lowest IC_{50} values for each drug tested. The early apoptosis marker eAnnexinV Green showed significant increases in signal with increased drug concentrations for all treatments except methotrexate (Figure 8B). Apoptotic signal IC_{50} values were generally higher than proliferation IC_{50} values, including two orders of magnitude higher for staurosporine. Irreversible cell death, evaluated through PI signal dose-response analysis, resulted in the highest IC_{50} values measured for each drug (Figure 8C). The observed IC_{50} effects were consistent with temporal and concentration-dependent sequential processes in which suppression of cell proliferation proceeded apoptotic events, which in turn either proceeded or coincided with committed cell death and irreversible loss of membrane integrity.

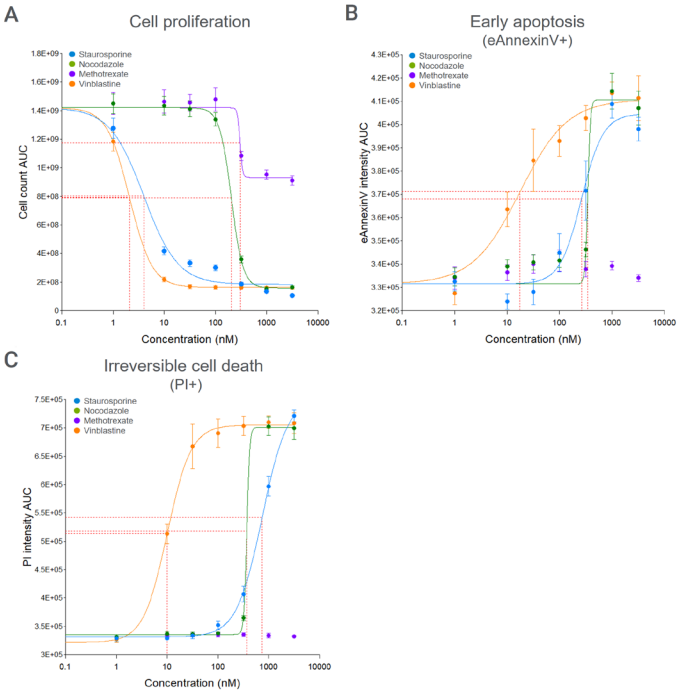

Figure 8. Dose-response analysis for drug effect on proliferation, early apoptosis and irreversible cell death. (A) Dose-response curves for four drugs impacting HT-1080 cell culture proliferation. Cell count area-under-the-curve (AUC) values were plotted against drug concentration and four-parameter fits (solid lines) were used to determine IC_{50} values (red dashed lines) for each drug in Agilent BioTek Gen5 software. Proliferation effect IC_{50} values correspond to 4.0 nM for staurosporine, 200 nM for nocodazole, 300 nM for methotrexate, and 2.0 nM for vinblastine. Data points represent mean and standard deviation for replicate wells (n = 10). (B) Dose-response analysis for apoptotic signal. Per cell mean eAnnexinV Green signal was normalized to control values. Normalized signal AUC values were plotted against drug concentration and four-parameter fits (solid lines) were used to determine IC_{50} values (red dashed lines) for each drug in Gen5 software. Apoptotic signal IC_{50} values correspond to 260 nM for staurosporine, 350 nM for nocodazole, and 18 nM for vinblastine. Methotrexate did not show a significant apoptotic response. Data points represent mean and standard deviation for replicate wells (n = 10). (C) Dose-response analysis for irreversible cell death signal. Per-cell mean PI signal was normalized to control values. Normalized signal AUC values were plotted against drug concentration and four-parameter fits (solid lines) were used to determine IC_{50} values (red dashed lines) for each drug in Gen5 software. Committed cell death signal IC_{50} values correspond to 740 nM for staurosporine, 370 nM for nocodazole, and 10 nM for vinblastine. Methotrexate did not show a significant committed cell death response. Data points represent mean and standard deviation for replicate wells (n = 10).

Scalability across high-throughput microplate formats

The Agilent BioTek Cytation 9 and BioSpa 8 automated platform is compatible with a variety of microplate formats supporting high-throughput proliferation and viability assays. Here, we provide example assays performed in both 96- and 384-well microplates that are commonly used for high-throughput cellular analysis (Figure 9). Low-magnification 4x imaging used for this assay results in a similar size culture region across both 384-well (Figure 9A) and 96-well microplate types (Figure 9E). Similar culture areas per image result in a similar number of cells identified and analyzed with Gen5 software image analysis (Figure 9B and F), leading to similar statistical strength across formats. The increased capacity inherent in a 384-well format (Figure 9C) provides the opportunity to increase the number of test conditions or the technical replicates assayed compared to 96-well formats (Figure 9G). Here, both 96- and 384-well formats ultimately demonstrated excellent agreement in analytical outcomes, as demonstrated by comparing dose-response analysis on proliferation effects and IC_{50} determination (Figure 9D and H).

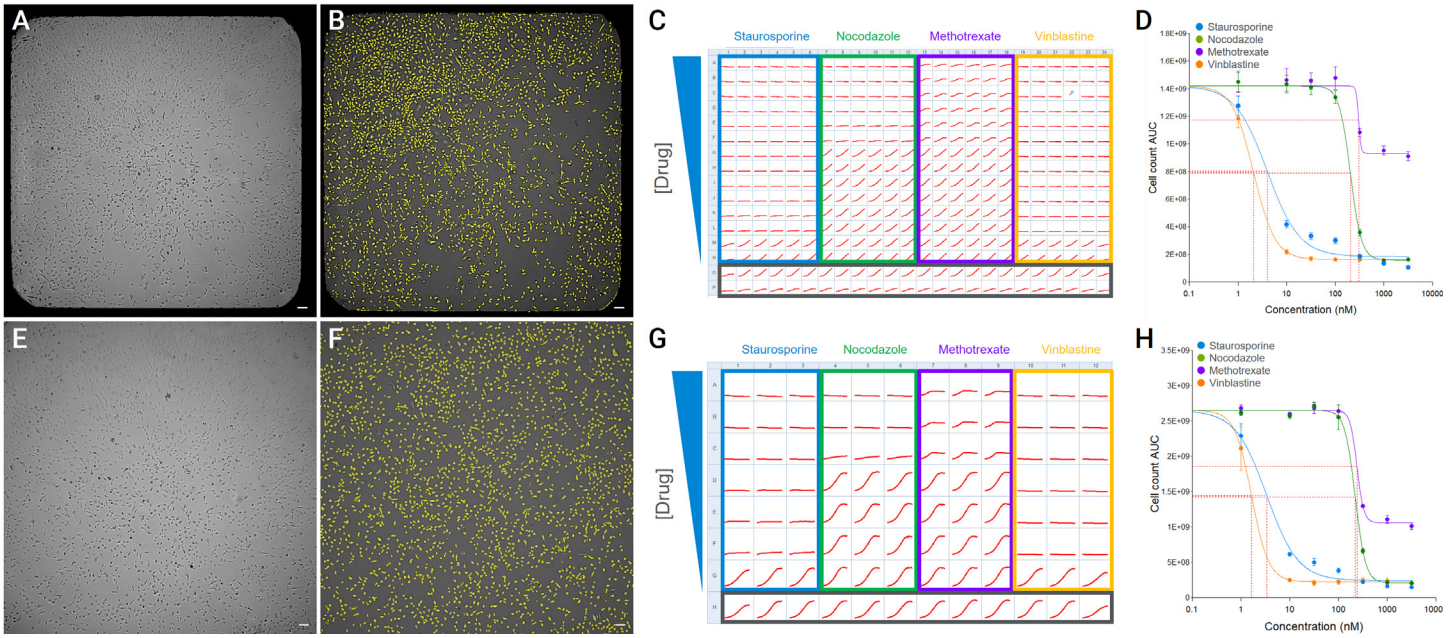

Figure 9. Flexible support for multiple high-throughput assay formats. (A) Example brightfield image of 384-well plate type at 4x magnification on the Agilent BioTek Cytation 9 cell imaging multimode reader. A single 4x magnification image provides whole-well analysis in 384-well microplates. (B) High-contrast cell counting image with cell identification (yellow overlay) with Agilent BioTek Gen5 software identified all the cells in the well. (C) Example plate overview for 384-well plate format displaying proliferation curves across the plate (red curves) and test compounds (blue, green, purple, and gold) and control wells (grey) in corresponding color outlines. (D) Proliferation dose-response analysis results for four test compounds in 384-well microplate format. Data points represent mean and standard deviation for replicate wells (n = 12). Proliferation effect IC_{50} values correspond to 4.0 nM for staurosporine, 200 nM for nocodazole, 300 nM for methotrexate, and 2.0 nM for vinblastine. (E) Example brightfield image from the center of a well from a 96-well plate type at 4x magnification on the Cytation 9 imaging reader. A single 4x magnification image captures ~ 40% of the total well area and a similar but slightly larger total culture area than 384-well plate types, as shown in panel A. (F) High-contrast cell counting image with cell identification (yellow overlay) with Gen5 software identified all the cells in the image. Scale bars correspond to 100 µm. (G) Example plate overview for 96-well plate format displaying proliferation curves across the plate (red curves) and test compounds (blue, green, purple, and gold) and control wells (grey) in corresponding color outlines. (H) Proliferation dose-response analysis results for four test compounds in 96-well microplate format. Proliferation effect IC_{50} values correspond to 3.4 nM for staurosporine, 220 nM for nocodazole, 240 nM for methotrexate, and 1.7 nM for vinblastine. Data points represent mean and standard deviation for replicate wells (n = 3).

Conclusions

The Agilent BioTek Cytation 9 and BioSpa 8 platform provide a fully automated, walk-away solution for long-term live-cell imaging, delivering faster acquisition speed, improved image quality, and consistent environmental stability across extended assays. The combination of label-free high-contrast brightfield imaging with multiplexed fluorescence markers enables parallel evaluation of cell proliferation and viability within the same experiment, supported by direct cell counts, normalized viability metrics, and information-rich images. This approach demonstrates robust performance across both 96- and 384-well microplate formats, with up to eight plates managed automatically through the BioSpa 8. The unified image acquisition and analysis interface in the Agilent BioTek Gen5 software integrates image segmentation, kinetic evaluation, and dose-response quantification, providing powerful analytical flexibility.

Together, these capabilities establish the Cytation 9 and BioSpa 8 system as a robust and scalable platform for comprehensive live-cell analysis. Automated multimode imaging, integrated analytical tools, and high-throughput capacity support a range of applications in drug discovery, oncology research, cytotoxicity profiling, and mechanism-of-action studies.

References

1. Hanahan, D. and Weinberg, R. A. The Hallmarks of Cancer: The Next Generation. *Cell* **2011**, *144*(5), 646–674. https://doi.org/10.1016/j.cell.2011.02.013
2. Segawa, K. and Nagata, S. An Apoptotic 'Eat Me' Signal: Phosphatidylserine Exposure. *Trends in Cell Biology* **2015**, *25*(11), 639–650. https://doi.org/10.1016/j.tcb.2015.08.003
3. Vermes, I.; Haanen, C.; Steffens-Nakken, H.; Reutelingsperger, C. A Novel Assay for Apoptosis: Flow Cytometric Detection of Phosphatidylserine Expression on Early Apoptotic Cells Using Fluorescein-Labelled Annexin V. *J Immunol Methods* **1995**, *184*, 39–51. https://doi.org/10.1016/0022-1759(95)00072-i
4. Gong, Y.; Fan, Z.; Luo, G.; Yang, C.; Huang, Q.; Fan, K.; Cheng, H.; Jin, K.; Ni, Q.; Yu, X. et al. The Role of Necroptosis in Cancer Biology and Therapy. *Mol Cancer* **2019**, *18*, 100. https://doi.org/10.1186/s12943-019-1029-8
5. Visentin, M.; Zhao, R.; Goldman, D. The Antifolates. *Hematol Oncol Clin North Am* **2012**, *26*, 629–48. https://doi.org/10.1016/j.hoc.2012.02.002

Products used in this application

Agilent products

BioTek Cytation 9 Cell Imaging Multimode Reader

BioTek BioSpa 8 Automated Incubator

BioTek BioSpa Live Cell Analysis System

BioTek Gen5 Software for Imaging & Microscopy

www.agilent.com/lifesciences/biotek

DE-013343

Published in the USA, March 16, 2026
5994-9060EN

Agilent